Scale-dependent fault roughness effects on earthquake dynamics and ground-motion

Thomas Ulrich and Alice-Agnes Gabriel

2020 SCEC annual meeting

LMU Munich, Germany

Summary

The effects of **fault roughness** on earthquake rupture dynamics and the radiated seismic wavefield have received increasing attention in numerical models aiming to capture **the full frequency range of observed ground motions**.

We investigate the **scale dependence** of fault roughness effects in terms of **rupture process zone width** and **minimum roughness wavelength** on earthquake kinematics, dynamics, and ground motion. We study **simple models of varying process zone width** and faults incorporating **band-limited roughness with varying length scales**. We find that a larger rupture process zone leads to less coherent rupture fronts and higher variability of rupture speed. In addition, **peak slip rate** distributions are systematically modulated by the process zone width, highlighting its importance in modulating fault roughness dynamic effects. However, the spectral content of fault slip and rupture speed is consistently self-similar over all scales.

We then discuss the choice of the **smallest wavelength** of the bandlimited rough fault geometry and propose an efficient hybrid approach combining meshed fault roughness, roughness drag and traction heterogeneities.

1. Methods

- **High-resolution 3D** dynamic rupture modeling using **SeisSol** : Seismic wave propagation coupled with frictional fault failure and off-fault inelasticity, optimized for high-performance computing. https://github.com/SeisSol/SeisSol
- **Simple models**: homogeneous medium, flat free surface, all models based on the same strike-slip band-limited self-similar rough fault (50 ✕ 15 km, minimum (resp. maximum roughness wavelength λ_{min} = 200m (resp. λ_{max} = 50km), α = 10^{-2}, Hurst index H=1).
- We use **linear slip weakening** friction because it is easier to control the rupture process zone width, e.g. using Day et al. (2005) breakdown-zone width estimate:

$$\Lambda_0^{III} = \frac{9\pi}{32}\mu\frac{D_c}{\tau_s - \tau_d}$$

With μ the shear modulus, D_c the slip weakening distance, $\boldsymbol{\tau}_s$ the fault shear strength and $\boldsymbol{\tau}_d$ the fault frictional resistance

- Stress is Andersonian, the angle of maximum compressive stress to the fault is 50°
- Off-fault plasticity (Wollherr et al., 2018) is accounted for, to prevent unrealistic stresses near the fault kinks.

2. Rough fault rupture dynamics with varied process zone width

- We simulate rupture of **varying process zone width** by varying Dc. The same fault is used in all simulations.
- Rupture evolution is controlled by the energy balance between strain energy release and fracture energy (Madariaga & Olsen 2000): all models have the same stress drop, but the **fault strength (parametrized by the prestress ratio R_0) is adapted** to keep this balance unchanged.
- Our results suggest that the dynamic rupture process zone width is a key factor modulating the strength of roughness effects. A **larger rupture process zone** leads to **less coherent rupture fronts** and **higher variability of rupture speed**.
- We observe a systematic change in the spectral fall-off of **peak slip rate** associated with the **process zone length** (Fig 4b) highlighting its importance in **modulating fault roughness dynamic effects**.
- On the other hand, the spectral content of **other rupture characteristics** (fault slip, rupture speed) **is consistently self-similar over all scales**, suggesting that such critical behavior is not an intrinsic characteristic of fault roughness effects.

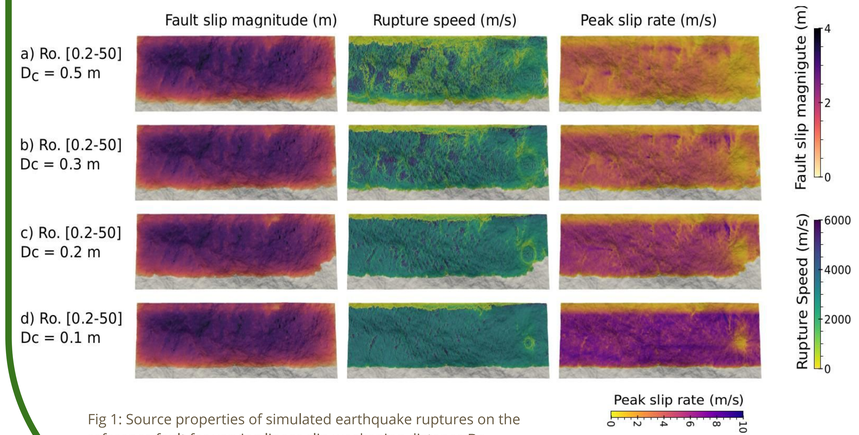

Fig 1: Source properties of simulated earthquake ruptures on the reference fault for varying linear slip weakening distance Dc

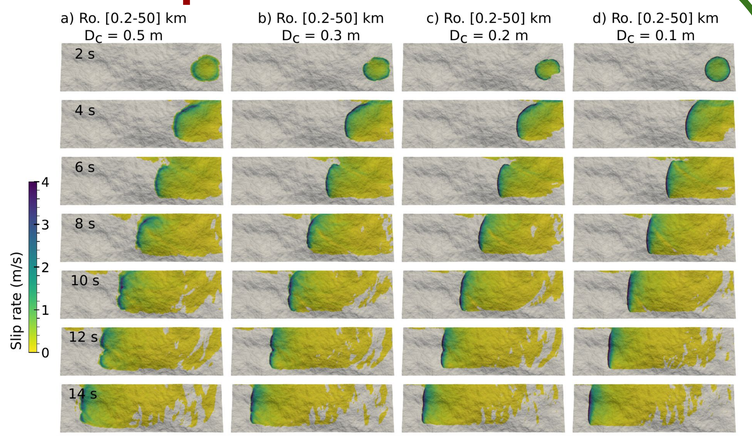

↑Fig 2: Overview of simulated earthquake ruptures on the reference fault for varying linear slip weakening distance Dc.

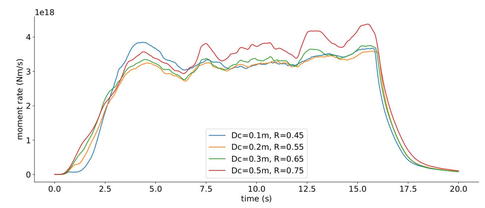

←Fig 3: Moment rate functions of simulated earthquake ruptures on the reference fault for varying linear slip weakening distance Dc.

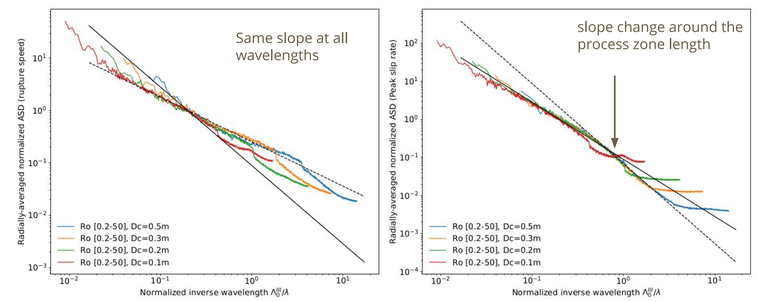

Fig 4: Normalized radially-averaged amplitude spectral density of the rupture speed (a) and the peak slip rate (b). The x axis is normalized by Day et al. (2005)'s estimate of the breakdown-zone with. All curves are normalized by their value at 0.2. The solid black lines illustrate the fall-off of a self-similar model (H=1). The dashed black lines illustrate the fall-off of a self-affine model featuring H=0.35 (a) (resp. H=1.6, (b)).

3. Heterogeneous tractions as a proxy for small-scale roughness

- The **numerical cost** of dynamic rupture models incorporating fault roughness effects may be greatly affected by the **choice of λmin.**
- Based on our findings, we develop strategies to **emulate** the full dynamic behavior **in a hybrid approach**, combining **small-scale** traction and strength **heterogeneity** with **larger-scale geometric complexity**.
- Rupture on a fault derived from a reference fault by **low-pass filtering** its smallest-scale geometric features can resemble the rupture on the reference fault if **fault strength is scaled** accordingly.

$$\tau_{\text{drag}} = 8\pi\alpha^2 G^* \Delta(1/\lambda_{\min} - 1/\lambda_{\max})$$

Roughness drag contribution of the filtered roughness bandwidth, with Δ the fault slip and α the amplitude to wavelength ratio (Fang and Dunham, 2013).

- Nevertheless, the fault slip, rupture velocity and peak slip rate of such model **lack of small-scale heterogeneity**, which may translate into less realistic synthetic ground motion.
- Proposed hybrid approach: roughness effectively meshed only to a given wavelength and smallest geometric features approximated by **traction heterogeneities**. performs better at capturing small-scale variations of fault slip and rupture velocity.

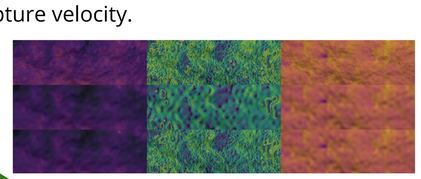

Fig 7: Zoomed view on part of the source properties (Fig. 6)

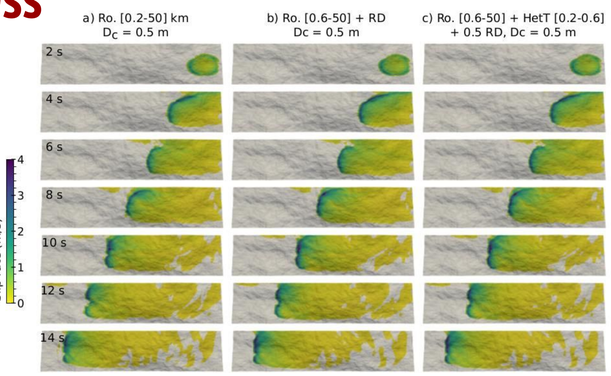

Fig 5: Overview of simulated earthquake ruptures on the reference fault (a) and on a fault derived (low-pass filtered) from the reference fault (b,c). (b) scaled strength (c) hybrid approach (traction heterogeneities and scaled strength).

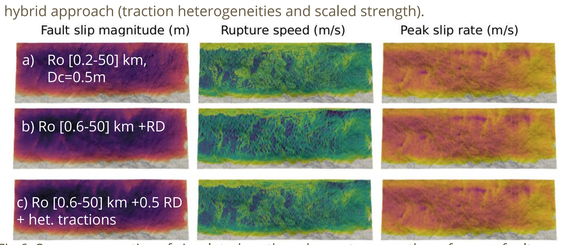

Fig 6: Source properties of simulated earthquake ruptures on the reference fault (a) and on a fault derived (low-pass filtered) from the reference fault (b,c). Rupture speed in (b) lacks of small-scale wavelengths.

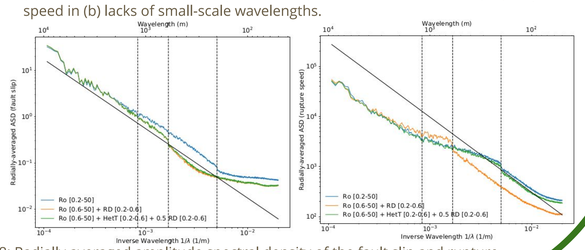

Fig 8: Radially averaged amplitude spectral density of the fault slip and rupture speed. The solid black lines illustrate the fall-off of a self-similar model (H=1).

4. Fault roughness and ground-motion

- Surprisingly, ruptures on both low-pass filtered and reference fault yield high-frequency (up to 10Hz) ground motion with a **high degree of statistical similarity** (e.g. Fig. 10)**.**
- The peak slip rate distribution has certainly a strong impact on the distribution of near-field ground motion. The fluctuations of the peak slip rate decay strongly for decreasing wavelengths below the process zone width (Fig. 4b). Models based on the derived fault, filtered of wavelengths smaller than the estimated process zone width, therefore **capture most of the peak slip rate fluctuations**, and then yield comparable ground motion.
- The simulated ground-motion presents a **flat spectrum** up to a **corner frequency** which **increases** with **decreasing process zone width**.
- The **spatial distribution** of the high frequencies ground-motion appears **independent of the process zone width** (Fig. 12: same H, no change of slope).

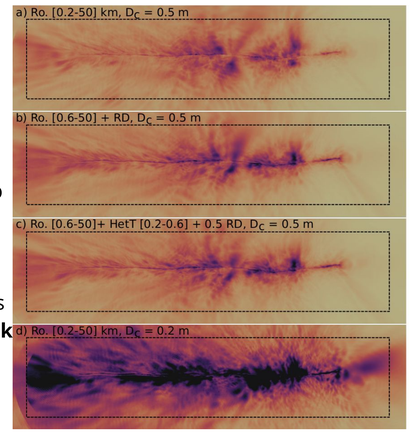

↑Fig 9: Near-field synthetic ground motion distribution: spectral acceleration computed at 9Hz.

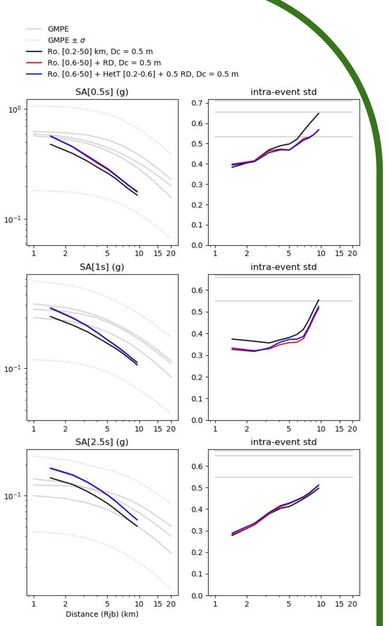

↗ Fig 10: comparison of synthetic near-field ground motion data with 4 recent ground motion prediction equations (GMPE). Left: average spectral acceleration at 0.5, 1 and 2.5s vs fault distance. Right: intra-event standard deviation vs fault distance.

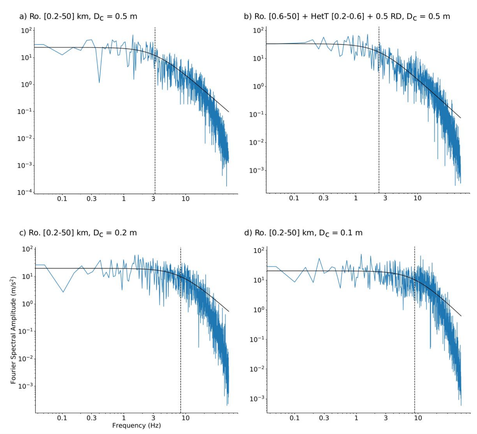

→Fig 11: Median acceleration spectrum along a line of 100 receivers spaced every 0.5km between x=-25 km and x=25 km at y=0 km (roughly above the fault). The black line corresponds to a omega-square model that best fits the data, and the dashed vertical line to its corner frequency.

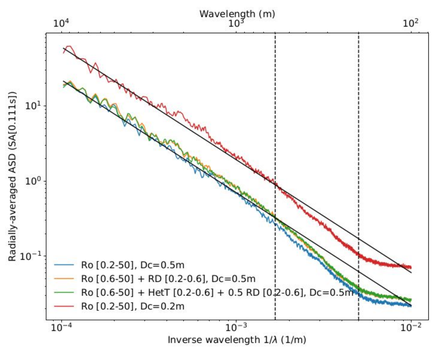

Fig 12: Radially-averaged amplitude spectral density of spectral acceleration at 9Hz SA[0.111s]. The black lines illustrate the fall-off of a self-similar model.

REFERENCES: Day, S. M., Dalguer, L. A., Lapusta, N., & Liu, Y. (2005). Comparison of finite difference and boundary integral solutions to three-dimensional spontaneous rupture. Journal of Geophysical Research: Solid Earth, 110(B12). Wollherr, S., Gabriel, A. A., & Uphoff, C. (2018). Off-fault plasticity in three-dimensional dynamic rupture simulations using a modal Discontinuous Galerkin method on unstructured meshes: implementation, verification and application. Geophysical Journal International, 214(3), 1556-1584. Madariaga, R., & Olsen, K. B. (2000). Criticality of rupture dynamics in 3-D. In Microscopic and macroscopic simulation: Towards predictive modelling of the earthquake process (pp. 1981-2001). Bruhat, L., Klinger, Y., Vallage, A., & Dunham, E. M. (2019). Influence of fault roughness on surface displacement: from numerical simulations to coseismic slip distributions.Fang, Z., & Dunham, E. M. (2013). Additional shear resistance from fault roughness and stress levels on geometrically complex faults. Journal of Geophysical Research: Solid Earth, 118(7), 3642-3654.